



HAL
open science

Combining a fractional diffusion equation and a fractional viscosity-based magneto dynamic model to simulate the ferromagnetic hysteresis losses

Benjamin Ducharne, G. Sebald

► **To cite this version:**

Benjamin Ducharne, G. Sebald. Combining a fractional diffusion equation and a fractional viscosity-based magneto dynamic model to simulate the ferromagnetic hysteresis losses. *AIP Advances*, 2022, 12 (3), pp.035029. 10.1063/9.0000254 . hal-03836245

HAL Id: hal-03836245

<https://hal.science/hal-03836245>

Submitted on 2 Nov 2022

HAL is a multi-disciplinary open access archive for the deposit and dissemination of scientific research documents, whether they are published or not. The documents may come from teaching and research institutions in France or abroad, or from public or private research centers.

L'archive ouverte pluridisciplinaire **HAL**, est destinée au dépôt et à la diffusion de documents scientifiques de niveau recherche, publiés ou non, émanant des établissements d'enseignement et de recherche français ou étrangers, des laboratoires publics ou privés.

Combining a fractional diffusion equation and a fractional viscosity-based magneto dynamic model to simulate the ferromagnetic hysteresis losses.

B. Ducharne*, G. Sebald

ELyTMaX UMI 3757, CNRS – Université de Lyon – Tohoku University, International Joint Unit, Tohoku University, Sendai, Japan.

* corresponding author: benjamin.ducharne@insa-lyon.fr

Abstract:

Magnetic losses in a laminated ferromagnetic core have been studied for years. However, magnetization mechanisms are complex, and the ideal model is still lacking. Classic resolution in the time domain combines a 1D magnetic diffusion equation with a viscosity-based magneto dynamic material law (first-order differential equation). This simultaneous resolution has already been solved by matrix inversion: the diffusion equation temporal term is replaced by its differential equation expression. It leads to a fast solution but overestimates the excess losses linked to the dynamic of the magnetic domains wall motions. Improved material laws using power operators have alternatively been tested. However, it is impossible to regroup the magnetic field terms on the same side of the final equation, and the resolution can only go through complex iterative methods (fixed point, Newton-Raphson). In this study, we propose to combine a fractional diffusion equation and a fractional viscosity-based magneto dynamic differential equation. Matrix resolution is possible, such as an accurate simulation of the dynamic behavior by adjusting the fractional order. The space term of the diffusion equation being solved by space discretization, the combined resolution leads to local information (excitation and induction fields). The number of dynamic parameters is limited but large enough for excellent simulation results.

Keywords:

Ferromagnetic losses, fractional derivative, local hysteresis

1 - Introduction:

Electromagnetic actuators and convertors are omnipresent in contemporary society. The magnetic core is a critical conversion element. An accurate evaluation of the conversion law is mandatory in the design of new electromagnetic devices. The first scientific work on this topic was published by Steinmetz more than a century ago [1]. Still, it is a timely issue, and the list of recent publications on this subject is simply breathtaking ([2]-[11] in less than a year). Zirka et al. in [12] wrote, “despite the long history of the problem and an undoubted requirement for its solution for numerous applications, it should be recognized that the general physical model of a ferromagnetic sheet has not yet been developed, not is likely to be developed in the foreseeable future.”

Among a vast list of publications, some should receive immediate attention, like the Steinmetz's empirical approach published at the end of the 19th century [1]. Seventy years later (1952), Polivanov [13], followed by Pry, and Bean [14], proposed the first qualitative models for the magnetization mechanisms. Even limited, these theories remained prevalent for many years up to Bertotti's Statistical Theory of Losses (STL), which is still nowadays the most used method to evaluate the ferromagnetic losses in electromagnetic conversions [15].

STL is based on the concept of losses separation. It works under sinusoidal magnetization and assumes the absence of skin effect (less than 150 Hz in typical electrical steels [16]). The total loss per cycle W_{tot} is supposed to be the sum of three contributions (Eq. 1):

$$W_{tot} = W_{hyst} + W_{clas} + W_{exc} \quad (1)$$

W_{hys} is the frequency-independent hysteresis loss contribution. W_{clas} (Eq. 2) is the classical eddy current loss term:

$$W_{cl} = \frac{\sigma d^2}{12} \int_0^{1/f} \left(\frac{dB_a}{dt} \right)^2 dt \quad (2)$$

W_{clas} is derived from Maxwell's equations, it is due to the macroscopic eddy currents. B_a is the projection of induction field \vec{B}_a averaged through the sheet cross-section in the \vec{O}_y direction (Fig.1). σ is the electrical conductivity, and d the lamination thickness. The last term W_{ex} is the excess eddy current loss (Eq.3), it is attributed to the magnetic domains kinetic as observed during the magnetization process.

$$W_{ex} = \sqrt{\sigma S G V_0} \int_0^{1/f} \left| \frac{dB_a}{dt} \right|^{1.5} dt \quad (3)$$

S is the cross-section, $G = 0.1356$ a dimensionless coefficient and V_0 a $Max(B)$ dependent statistical parameter linked to the microstructure. STL is a powerful tool, but it is a lumped method. Its application frequency range is limited, and it cannot be solved in the time domain.

Based on STL limitations, alternative methods were proposed. Among them, the simultaneous resolution of the Maxwell diffusion equation (Eq.4) and a viscosity-based magneto dynamic material law gave the most accurate results [17].

$$\nabla^2 \vec{H} = \sigma \frac{d\vec{B}}{dt} \quad (4)$$

Where \vec{H} is the magnetic excitation field. In a laminated ferromagnetic core and for geometrical reasons, it is common to reduce Eq.4 to the thickness dimension (1D). \vec{B} and \vec{H} being always parallel to the lamination direction, both these vectors quantities can be reduced to their scalar projection:

$$\frac{\partial^2 H(z,t)}{\partial z^2} = \sigma \frac{dB(z,t)}{dt} \quad (5)$$

Eq.5 left member is classically discretized through finite differences leading to local information.

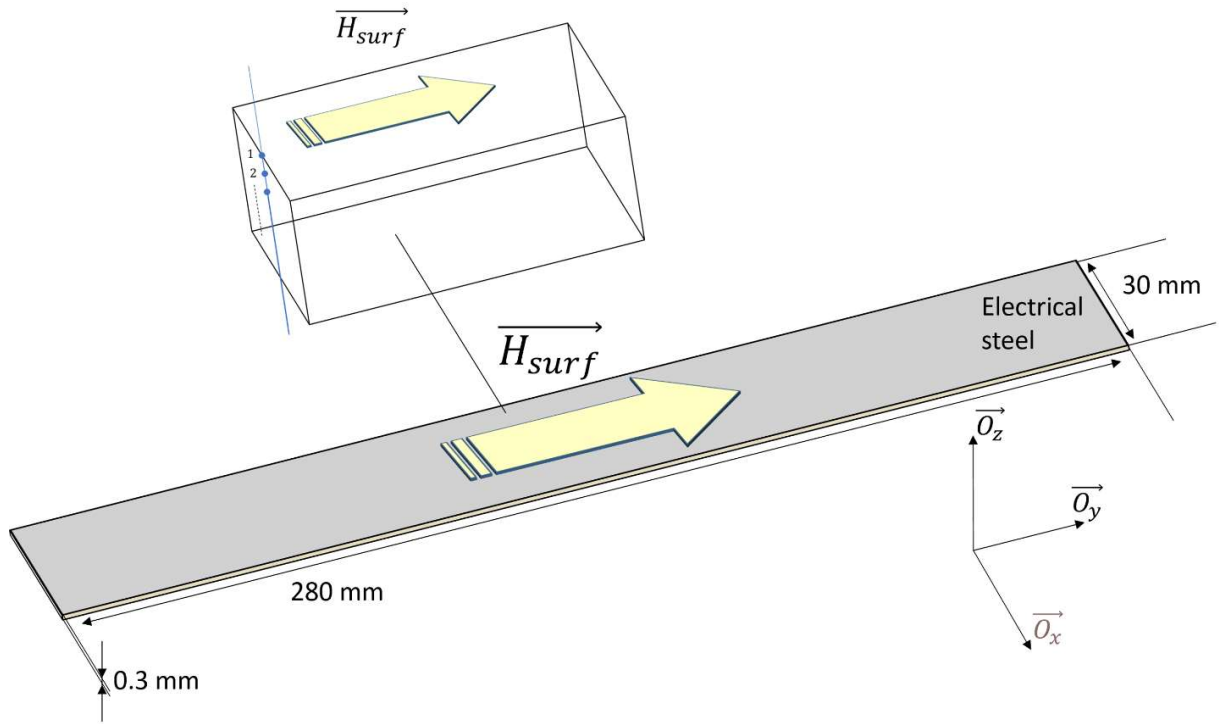


Fig.1 – Ferromagnetic electrical steel lamination: 1D space discretization and geometrical information.

Eq.5 is impossible to be solved in itself, and resolution can only be obtained by coupling it to a material law. For this, viscosity-based magneto dynamic differential equations are promoted [17][18], the simplest being:

$$\rho \left(\frac{dB(z,t)}{dt} \right) = H(z,t) - f_{static}^{-1}(B(z,t)) \quad (6)$$

Where ρ can be a constant or a B dependent function for better accuracy (see Eq.8), and $f_{static}^{-1}(B(z,t))$ a frequency-independent contribution calculated from a quasi-static hysteresis model (like the J-A model or the Preisach model in their inverse configuration $B(H)$ [19]).

A strong formulation (Eq.7) can be written by isolating $dB(z,t)/dt$ in both equations (Eq.5 and 6):

$$\frac{\partial^2 H(z,t)}{\partial z^2} = \sigma \frac{H(z,t) - f_{static}^{-1}(B(z,t))}{\rho} \quad (7)$$

Eq.7 can be solved by matrix inversion without an iterative method by moving all the $H_i(z, t)$ terms to the same side of the equation. Like this, Eq.7's resolution is fast and always convergent. Unfortunately, Eq.7 overestimates the magnetic losses in the high-frequency range as it inappropriately considers the excess losses.

In [12], much better results are obtained with the viscosity-based magneto dynamic differential equation given below:

$$\frac{dB}{dt} = \frac{\delta}{g(B)} |H(t) - H_{stat}(B)|^{\alpha(B)} \quad (8)$$

Where δ is a directional parameter (= +/- 1) and the B 's dependent functions $\alpha(B)$ and $g(B)$ are set by comparison with experimental results. The matrix inversion-type resolution is unfortunately forbidden in this configuration as it is impossible to regroup all the $H(z, t)$ terms on the same side of the equation. Thus, in [12], the combined resolution is obtained using the iterative Newton-Raphson method associated with the TriDiagonal-Matrix Algorithm (TDMA). Such a high number of parameters lead to excellent simulation results, but many limitations remain, including:

- the $\alpha(B)$ and $g(B)$ identification
- the convergency of the iterative methods

2 - fractional derivative method

Fractional derivative operators have already been used for the simulation of the magnetic losses in a laminated ferromagnetic core. Different mathematical methods have been tested so

far (fractional diffusion equation [19], fractional differential equation [20][21], lump model [22]), and accurate results were always obtained on broad frequency bandwidths.

The fractional diffusion equation can be derived from eq.5:

$$\frac{\partial^2 H(z,t)}{\partial z^2} = \sigma \frac{d^n B(z,t)}{dt^n} \quad (9)$$

This equation is somehow connected to the generalized fractional Maxwell equations. Still, their relations need to be established, so is their physical meaning.

Similarly, the fractional differential equation can be derived from eq.6.

$$\rho \left(\frac{d^n B(z,t)}{dt^n} \right) = H(z,t) - f_{static}^{-1}(B(z,t)) \quad (10)$$

All the fractional derivative methods exhibit a common feature. They all come from a classic magnetic losses simulation method where the first-order time derivative term was replaced with a fractional derivative one. Time fractional derivatives are suggested in the context of long-time heavy tail decays. The totality of the history is involved in a time t fractional derivative resolution. Time fractional derivatives are well suited to ferromagnetic hysteresis, in which real-time behavior is strongly dependent on the specimen history. The fractional derivative order constitutes an additional degree of freedom that can be adjusted to precisely fit the experimental results.

Just like Eq.5 and 6 have been regrouped in Eq.7, if n in Eq.9 and Eq.10 is equal, their fractional versions can be rearranged the same way:

$$\frac{d^n B(z,t)}{dt^n} = \frac{1}{\sigma} \frac{\partial^2 H(z,t)}{\partial z^2} = \frac{H(z,t) - f_{static}^{-1}(B(z,t))}{\rho} \quad (11)$$

Then, Eq.11's space term can be discretized in 1D using finite differences (see Fig.1, for the node distribution), and the whole equation is solved through matrix inversion (Euler's method) as described in [17]:

$$[M] \cdot [H] = [S_1] + [S_2] \quad (12)$$

Here, [M] is the stiffness matrix made out of constant terms, [H] includes the unknown excitation fields, and [S₁], [S₂] are defined as:

$$[S_1] = \begin{bmatrix} H_{surf} \\ 0 \\ \vdots \end{bmatrix} \quad [S_2] = \begin{bmatrix} \frac{\sigma e^2}{\rho} \cdot H_{1stat}(B_1) \\ \frac{\sigma e^2}{\rho} \cdot H_{2stat}(B_2) \\ \vdots \end{bmatrix} \quad (13)$$

For each simulation time step, the determination of [H] is followed by a local calculus of $B(z, t)$, resolution of Eq.14 for every node of the mesh:

$$B_i(t) = \frac{d^{-n} \left(\frac{H_i(t) - f_{static}^{-1}(B_i(t))}{\rho} \right)}{dt^{-n}} \quad (14)$$

Eventually, $B_a(t)$ is calculated by averaging all $B_i(t)$ through the specimen cross-section:

$$B_a(t) = \frac{\sum_1^p B_i(t)}{p} \quad (15)$$

Where p is the number of space discretization.

3 – Comparison to experimental results

The measurement of the magnetic losses in a magnetic lamination is described by international standards [23][24]. For the classic Epstein frame method [23], the reproducibility standard deviation must be maintained lower than 1.5% up to 1.5 T for non-oriented electrical steels and up to 1.7 T for oriented ones.

Similarly, the reproducibility of the magnetic behavior of same-grade electrical steel is far from ensured by the manufacturer. In [25], for instance, the test values are supposed to be typical but not guaranteed.

The accumulation of the characterization setup's and the specimen behavior's uncertainties makes access to reliable and comparable experimental data hazardous. For all these reasons, we opted for already published experimental results [22], instead of engaging in a new testing campaign. The specimens tested were grain-oriented electrical steel (FeSi 3 wt% GO) sheets of thickness 0.22 mm and conductivity $2 \cdot 10^6 \text{ S}\cdot\text{m}^{-1}$. We refer readers to the original document [22] for additional information, including the experimental conditions.

In Fig.2 below, simulated and measured W_{tot} are compared for increasing values of $\max(B_a)$ and increasing value of the frequencies. Some local simulated hysteresis cycles $H_i(B_i)$ are plotted for different amplitude and frequency conditions. The simulation method described in section 2 works under $H_{surf}(t)$ imposed conditions, however following the international standards recommendations, all measurements were obtained under sinus $B_a(t)$ imposed conditions. Therefore, an inversion of the simulation method was performed, we opted for an explicit approach, by testing a H_{surf} 's window for every simulation step time and conserving the value minimizing the difference between the simulation and the targeted imposed $B_a(t)$. J-A⁻¹ was used for the quasi-static hysteresis contribution. The dynamic simulation parameters were set through the minimization of an uncertainty function (Eq.16):

$$Uncertainty (\%) = \frac{100}{q} \sum_{i=1}^q \frac{|W_{meas_i} - W_{sim_i}|}{W_{meas_i}} \quad (16)$$

Where q was the number of time discretization, all the simulation parameters are given in Tab.1.

Ten nodes were used for the half thickness as we noticed that from ten and beyond the influence of the space discretization was imperceptible. Also, a minimum of a hundred timesteps per period was required to obtain consistent simulation results.

Tab.1 –Simulation parameters.

| Static contribution parameters | | Dynamic contribution parameters | |
|--------------------------------|-------------------|---------------------------------|---------------|
| J-A ⁻¹ Parameters | Typical value | | Typical value |
| a (A.m ⁻¹) | 6 | ρ | 0.044 |
| Ms (A.m ⁻¹) | 1353000 | n | 0.83 |
| k (A.m ⁻¹) | 19 | | |
| c | 0.15 | | |
| α | $8 \cdot 10^{-6}$ | | |

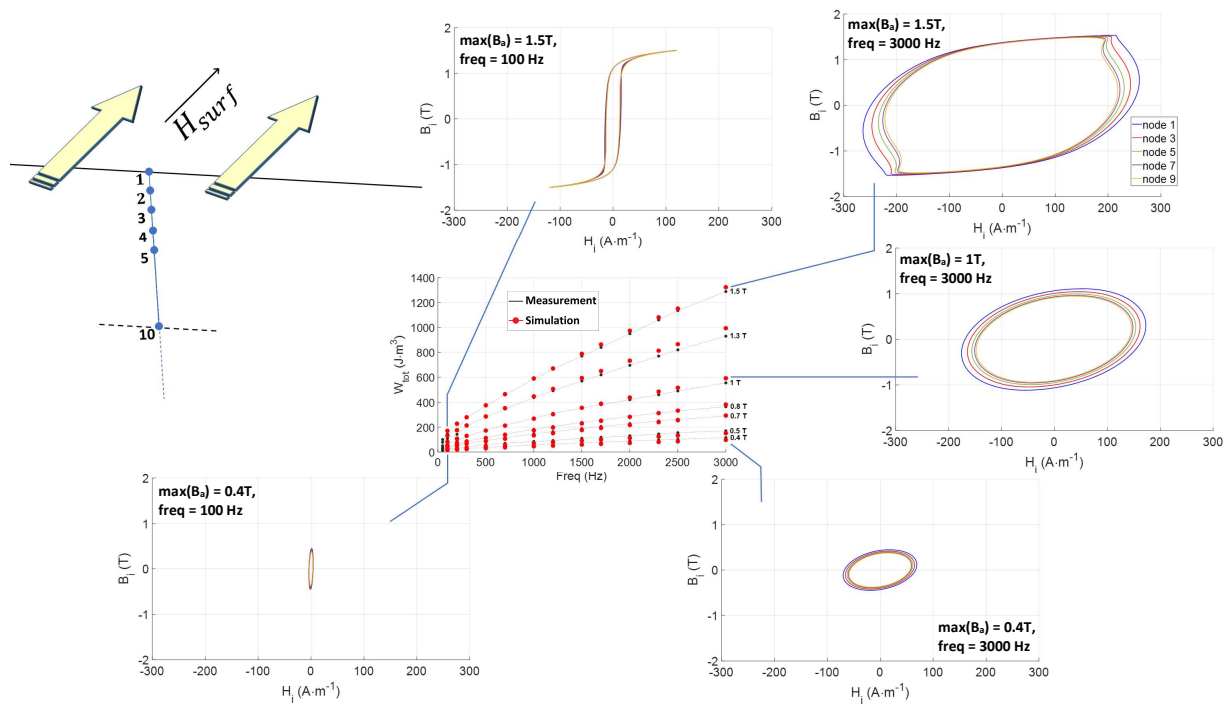
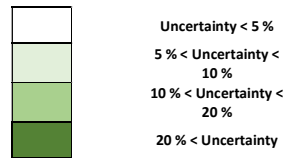


Fig.2 – Comparison simulation/measurement for W_{tot} , and simulated local hysteresis cycles for different amplitude and frequency conditions.

Tab.2 summarizes quantitatively the simulation methods accuracy. An approximated 6.7 % uncertainty was reached. The simulation times were lower than a second for a 1000 timestep discretization.

Tab.2 – W_{tot} uncertainty for all the experimental situations tested.

| Freq (Hz) | 50 | 100 | 200 | 300 | 500 | 700 | 1000 | 1200 | 1500 | 1700 | 2000 | 2300 | 2500 | 3000 | Uncertainty (%) |
|----------------------------|-------|-------|------|-------|-------|-------|-------|-------|-------|-------|-------|-------|-------|-------|-----------------|
| B_{MAX} (T) | | | | | | | | | | | | | | | |
| 0.4 | 28.30 | 27.70 | 0.00 | 9.30 | 9.00 | 11.70 | 12.60 | 13.60 | 12.10 | 13.60 | 13.40 | 13.10 | 12.90 | 10.68 | 13.43 |
| 0.5 | 12.50 | 10.00 | 0.00 | 16.60 | 14.20 | 12.90 | 9.70 | 12.70 | 11.80 | 10.70 | 12.40 | 12.90 | 8.80 | 9.50 | 11.05 |
| 0.7 | 16.60 | 19.50 | 2.80 | 4.30 | 6.10 | 8.20 | 7.00 | 5.80 | 5.80 | 4.80 | 3.20 | 3.00 | 1.70 | 1.81 | 6.47 |
| 0.8 | 18.60 | 20.60 | 0.50 | 2.50 | 4.80 | 4.10 | 3.60 | 6.10 | 2.70 | 1.90 | 0.10 | 0.60 | 4.60 | 1.28 | 5.14 |
| 1 | 3.00 | 4.50 | 8.00 | 9.70 | 8.80 | 6.60 | 7.00 | 3.60 | 1.80 | 0.40 | 1.90 | 2.00 | 3.90 | 3.49 | 4.62 |
| 1.3 | 0.00 | 5.60 | 9.10 | 7.40 | 4.90 | 3.40 | 2.00 | 0.10 | 0.90 | 1.70 | 2.40 | 2.50 | 4.30 | 4.49 | 3.49 |
| 1.5 | 3.40 | 15.00 | 5.80 | 4.00 | 3.40 | 2.50 | 2.20 | 0.30 | 0.00 | 0.30 | 0.00 | 0.40 | 0.90 | 3.34 | 2.97 |
| Uncertainty (%) | 11.77 | 14.70 | 3.74 | 7.69 | 7.31 | 7.06 | 6.30 | 6.03 | 5.01 | 4.77 | 4.77 | 4.93 | 5.30 | 4.94 | 6.74 |



It is worth noting in Fig.2, the evolution of the local hysteresis cycles. As expected, these cycles exhibit a similar shape in the low-frequency range and diverge at 3 kHz. However, this divergence is relatively weak and can be interpreted as a limited contribution of the macroscopic eddy currents, which can be justified as a combination of the laminated ferromagnetic core size and the relatively low electrical conductivity of the FeSi 3wt% GO electrical steel.

4 – Conclusion

The performance of electromagnetic devices depends mainly on their magnetic energy conversion efficiency. The adequate modeling of this efficiency is essential in device design processes. The present work addressed the absence of a simulation method that yields

satisfactory modeling results for ferromagnetic materials on large frequency bandwidth and large amplitude variations.

By combining a fractional diffusion equation with a fractional viscosity-based magneto dynamic law, the authors defined a very efficient simulation method. This model can be solved simply through matrix inversion. It gives local information and offers sufficient adjustable parameters to allow excellent simulation results in a wide range of experimental situations.

As no iterative resolution is required, convergency is ensured, and explicit inversion can be performed to obtain sinus-type imposed B_a simulation results as imposed by the characterization standards. The finite difference discretization of the diffusion equation space term gives access to local information and provides interesting information regarding the macroscopic eddy current generation and distribution.

Tab.3 below summarizes the pros and cons of the most classical methods for the core loss simulation, including the technique described in this manuscript.

Tab.3 – Comparative study of the core loss simulation methods

| | Steinmetz's empirical formula [1] | Bertotti's statistical theory of losses [15] | Combination diffusion equation / simple viscosity-based magneto dynamic differential equation [17] | Combination diffusion equation / advanced viscosity-based magneto dynamic differential equation [12] | Combination fractional diffusion equation / fractional viscosity-based magneto dynamic differential equation |
|--------------------------------|-----------------------------------|--|--|--|--|
| Time domain / Frequency domain | Frequency domain | Frequency domain | Time domain | Time domain | Time domain |
| Simulation speed | ++ | ++ | + | - | + |
| Accuracy | -- | - | - | ++ | ++ |
| Number of parameters | + | + | + | - | + |
| required experimental data | - | + | + | - | + |

This study is limited to the FeSi 3wt% GO electrical steel, but different materials will be tested in the near future. The restriction to laminated core-type geometry will also be overcome by extending the method to toroidal or even unsymmetrical geometries.

References:

- [1] C.P. Steinmetz, "On the law of hysteresis," AIEE Trans., vol. 9, pp. 3 – 64, 1892. Reprinted under the title "A Steinmetz contribution to the AC power revolution," Introduction by J.E. Brittain, Proc. IEEE, vol. 72, n° 2, pp. 196 – 221, 1984.
- [2] H. Zhao, H. H. Eldeeb, Y. Zhang, D. Zhang, Y. Zhan, G. Xu, O. A. Mohammed, "An improved core loss model of ferromagnetic materials considering high-frequency and non-sinusoidal supply," *IEEE Trans. Ind. App.*, 2021.
- [3] C. S. Schneider, S.D. Gedney, N. Ojeda-Ayala, M.A. Travers, "Dynamic exponential model of ferromagnetic hysteresis," *Phys. B: Cond. Mat.*, vol. 607, 421802, 2021.
- [4] I. Sirotic, M. Kovacic, S. Stipetic, "Methodology and measurement setup for determining PWM contribution to iron loss in laminated ferromagnetic materials," *IEEE Trans. Ind. App.*, 2021.
- [5] B. Ducharne, P. Tsafack, Y.A. Tene Deffo, B. Zhang, G. Sebald, "Anomalous fractional magnetic field diffusion through cross-section of a massive toroidal ferromagnetic core," *Com. in Nonlin. Sci. and Num. Sim.*, vol. 92, 105450, 2021.
- [6] M. Elyoussef, S. Clenet, A. Vangorp, A. Benabou, P. Faverolle, J.C. Mipo, "Improving global ferromagnetic characteristics of laminations by heterogenous deformation," *IEEE Trans. En. Conv.*, 2021.
- [7] X. Zhao, H. Xu, Z. Cheng, Z. Du, L. Zhou, D. Yuan, "A simulation method for dynamic hysteresis and loss characteristics of GO silicon steel sheet under non-sinusoidal excitation," *IEEE Trans. App. Supercond.*, 2021.
- [8] P. Guo, W. Huang, W. Guo, L. Weng, "High frequency losses calculating model for magnetostrictive materials considering variable DC bias," *IEEE Trans. Mag.*, 2021.
- [9] R. Corcolle, L. Daniel, "3-D semi-analytical homogenization model for soft magnetic composites," *IEEE Trans. Mag.*, vol. 57, n°7, pp. 1 – 4, 2021.
- [10] K. Li, Z. Zhang, P. Wang, Y. Liu, J. Zeng, "A novel 3D simulation prediction model of mechanical properties of ferromagnetic materials via increment permeability method," *J Magn. Magn. Mat.*, vol. 536, 168137, 2021.
- [11] S. Zhang, B. Ducharne, S. Takeda, G. Sebald, T. Uchimoto, "Identification of the ferromagnetic hysteresis simulation parameters using classic non-destructive testing equipment," *J Magn. Magn. Mat.*, vol. 531, 167971, 2021.
- [12] S. E. Zirka, Y. I. Moroz, P. Marketos, A. J. Moses, "Viscosity-based magnetodynamic model of soft magnetic materials," *IEEE Trans. Mag.*, vol. 42, n° 9, pp. 2121 - 2132, 2006.

- [13] K. M. Polivanov, "Dynamic characteristics of ferromagnets," *Izv. Akad. Nauk SSSR, Ser. Fiz.*, vol. 16, pp. 449–464, 1952.
- [14] R. H. Pry and C. P. Bean, "Calculation of the energy loss in magnetic sheet materials using a domain model," *J. Appl. Phys.*, vol. 29, pp. 532–533, 1958
- [15] G. Bertotti, "General properties of power losses in soft ferromagnetic materials," *IEEE Trans. Magn.*, vol. 24, n° 1, pp. 621 – 630, 1988.
- [16] A. Broddefalk, M. Lindenmo, "Dependence of the power losses of a non-oriented 3% Si-steel on frequency and gaude," *J. of Mag. and Mag. Mat.*, Vol. 304, pp. 586-588, 2006.
- [17] M.A. Raulet, B. Ducharne, J.P. Masson and G. Bayada, "The magnetic field diffusion equation including dynamic hysteresis: a linear formulation of the problem," *IEEE Trans. Magn.*, vol. 40, n° 2, pp. 872 – 875, 2004.
- [18] B. Gupta, B. Ducharne, G. Sebald, T. Uchimoto, "A space discretized ferromagnetic model for non-destructive eddy current evaluation", *IEEE Trans. on. Mag*, Vol. 54, Iss. 3, 2018.
- [19] B. Ducharne, Y.A. Tene Deffo, B. Zhang, G. Sebald, "Anomalous fractional diffusion equation for magnetic losses in a ferromagnetic lamination," *The European Physical Journal Plus*, 135:325, 2020.
- [20] B. Zhang, B. Gupta, B. Ducharne, G. Sebald, T. Uchimoto, "Preisach's model extended with dynamic fractional derivation contribution," *IEEE Trans. Magn.*, Vol. 54, n° 3, pp. 1 – 4, 2018.
- [21] B. Zhang, B. Gupta, B. Ducharne, G. Sebald, T. Uchimoto, "Dynamic magnetic scalar hysteresis lump model, based on Jiles-Atherton quasi-static hysteresis model extended with dynamic fractional derivative contribution," *IEEE Trans. Magn.*, vol. 54, n° 11, pp. 1 – 4, 2018.
- [22] R. Liu, L. Li, "Analytical prediction of energy losses in soft magnetic materials over broadband frequency range," *IEEE Trans. Power Electron.*, vol. 36, n° 2, pp. 2009 – 2017, 2021.
- [23] IEC 60404-2, "Magnetic materials – Part 2: Methods of measurement of the magnetic properties of electrical steel strip and sheet by means of an Epstein frame," *International Electrotechnical Commission*, June 2008.
- [24] IEC 60404-3, "Magnetic materials – Part 3: Methods of measurement of the magnetic properties of electrical steel strip and sheet by means of a single sheet tester," *International Electrotechnical Commission*, April 2010.
- [25] "JFE steel corporation catalogue: Electrical steel sheets JFE G-CORE, JFE N-CORE," Japan, 2003.